2021

STUDYING THE EFFECTS OF INITIAL CRACK ANGLE ON THE CRACK PROPAGATION IN GRAPHENE NANO-RIBBON THROUGH MOLECULAR DYNAMICS SIMULATIONS

Vijay Kumar Pathak
Michigan Technological University, vpathak@mtu.edu

STUDYING THE EFFECTS OF INITIAL CRACK ANGLE ON THE CRACK PROPAGATION IN GRAPHENE NANO-RIBBON THROUGH MOLECULAR DYNAMICS SIMULATIONS

By

Vijay Kumar Pathak

A REPORT

Submitted in partial fulfillment of the requirements for the degree of

MASTER OF SCIENCE

In Mechanical Engineering

MICHIGAN TECHNOLOGICAL UNIVERSITY

2021

This report has been approved in partial fulfillment of the requirements for the Degree of MASTER OF SCIENCE in Mechanical Engineering.

Department of Mechanical Engineering - Engineering Mechanics

Report Advisor: *Dr. Susanta Ghosh*

Committee Member: *Dr. Dibakar Datta*

Committee Member: *Dr. Vijaya V. N. Sriram Malladi*

Department Chair: *Dr. William W. Predebon*

Dedication

To my mother, teachers and friends

who didn't hesitate to criticize my work at every stage - without which I would neither be who I am nor would this work be what it is today.

Contents

List of Figures

List of Tables

Acknowledgments

I would like to first thank my advisor, Dr. Susanta Ghosh, for formulating the research topic for me and for helping me with everything, by providing necessary resources and constant guidance. I have learned a lot from Dr. Ghosh and his passion for learning has certainly ignited an eternal knowledge-seeking flame within me.

I would like to thank Dr. Dibakar Datta for teaching me how to perform MD simulation and the theory behind it. Your constant support and knowledge-sharing have helped me a lot in getting this work done.

I would also like to thank Dr. Sriram Malladi for his support as a committee member. I would like to thank my research group members, especially Upendra Yadav for his initial guidance regarding the use of computational resources and Shashank Pathrudkar for his constant feedback on this work as it will continue.

In addition, I would like to thank Michigan Technological University for all the resources I have utilized to complete my report. I have used the HPC facility (Superior) at Michigan Tech for all my simulations, so I want to thank them separately.

I would like to thank all those who have helped me learn, understand and appreciate this subject as well as those who helped me with LaTeX.

Abstract

In this research, we have worked on the brittle fracture of graphene nano-ribbon to explore the behavior of crack propagation at different crack angles. We have performed classical Molecular Dynamics simulations using LAMMPS at ten different crack angles between 0 degrees and 45 degrees, in an increment of 5 degrees to observe the parameters that dominate the crack path. The graphene nanoribbon is loaded in the zigzag direction by pulling it in the armchair direction with a pre-existing crack in the center. We have used OVITO for the visualization of the simulation. AIREBO potential is employed in this work because it is extensively used in the fracture of graphene with different loading conditions and temperatures. The crack path is determined for all ten nanoribbons and the nanoribbon with a crack at 25° turned out to be the weakest because of the sharp crack tip and crack shape. The results are validated with the published results and are in accordance with them.

Chapter 1

Introduction

1.1 Graphene

In this age, when there is a huge requirement for synthesized materials of specific material properties, Graphene has become popular because it is the strongest known material. Not only it has excellent mechanical properties [3], but it also has very high thermal conductivity [4] (potentially a high-demand material in the semiconductor industry) and optical properties [5].

Graphene is a single layer of carbon atoms arranged in a honeycomb manner. This honeycomb shape enables a material to have minimal density and relatively high out-of-plane compression and shear properties.[6]

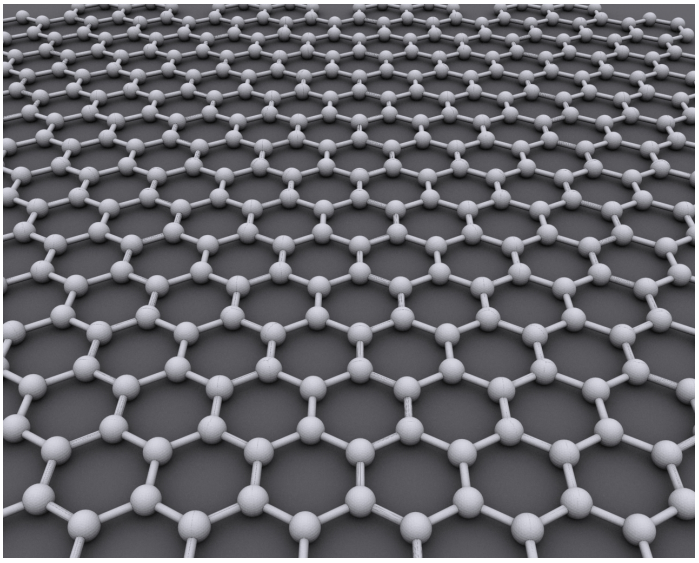

Figure 1.1: Honeycomb structure of monolayer graphene. Figure taken from [1]

This is one of the reasons why it has Young's Modulus of 1 Terapascal and intrinsic strength of 130 Gigapascals.[3] It is a super-material and can be used in multiple industries like biomedical, composites, electronics, sensors, energy, etc.

1.2 Molecular Dynamics

Molecular Dynamics is the study of movements of atoms/molecules which is performed through a computer simulation. It is employed for studies in the area of material science, biophysics, chemical physics, etc. It is the calculation of trajectories of atoms using Newton's equations of motion. All interactions between different atoms in a system are given in an interatomic potential, which is used to calculate

the forces between atoms and potential energies of the atoms.[7]

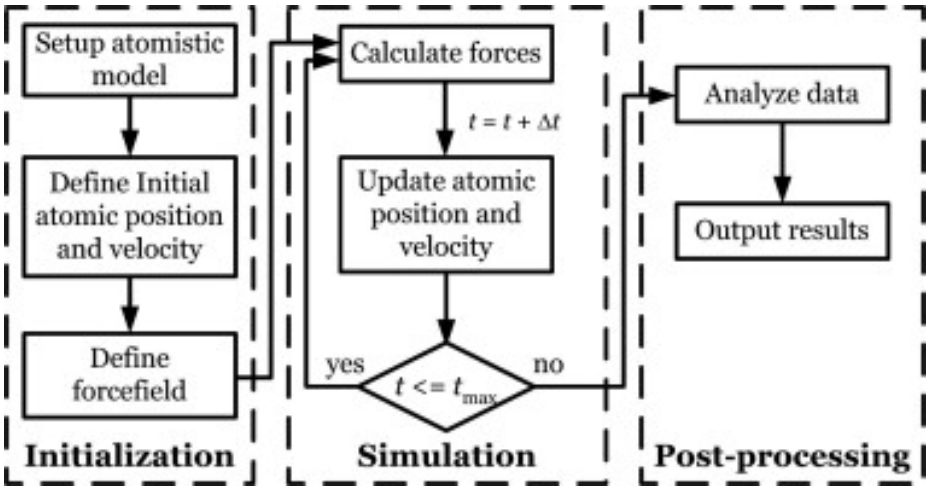

Figure 1.2: Schematic of a Molecular Dynamics simulation. Figure taken from [2]

In the initialization part, first, the atomistic model (geometry) is set up and then the model is defined through an input file that contains information such as boundary conditions, temperature, timesteps, etc. The forcefield is a mathematical function that calculates the potential energy of atoms in a system using their location.

In the simulation part, force is calculated by differentiating the total energy with respect to atomic locations, and the atomic locations and velocities are updated. It keeps on calculating forces and updating atomic locations and velocities until a maximum number of timesteps are reached. In the post-processing part, data is analyzed and then output results are visualized using visualization tools.

Chapter 2

Theory and Practice

This work is based on Datta et al.[8], only the crack geometry is slightly changed and the set of angles considered. We have used LAMMPS (Large-scale Atomic/Molecular Massively Parallel Simulator) to perform molecular simulations.[9] The dump files from LAMMPS are then used to visualize our results in OVITO.[10]

In this work, we have taken a graphene nanoribbon(GNR) of size 150×150 A$^\circ$ with a pre-crack of half-length 15 A$^\circ$(a_0) and it is tensile loaded in the armchair direction (zigzag graphene).[11] The number of carbon atoms is 8870. It is a 2D simulation, so the z velocity of the atoms is fixed, and to make this a non-periodic simulation, periodic boundary conditions are taken along with a larger size of the simulation box so that the atoms do not cross the boundary. This is depicted in Figure 2.1.

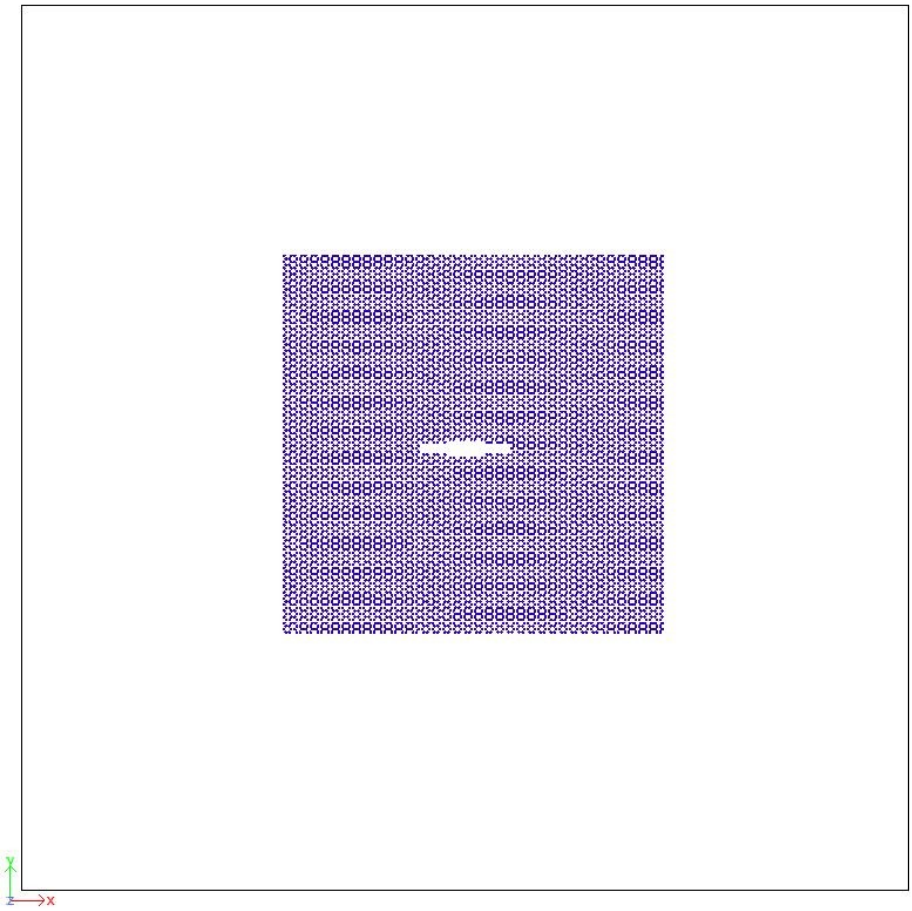

Figure 2.1: GNR inside the simulation box with a pre-crack oriented at 0°. The x and y axes correspond to the horizontal and vertical axes respectively.

2.1 LAMMPS

To perform any MD simulation, typically three files are required. They are input files, data files, and potential files. The data file is visualized in the Figure 2.1 and 2.2. Figure 2.2 also shows two orientations of graphene: armchair and zigzag. In this work, the GNR is pulled in the armchair direction, so that makes it loaded in zigzag

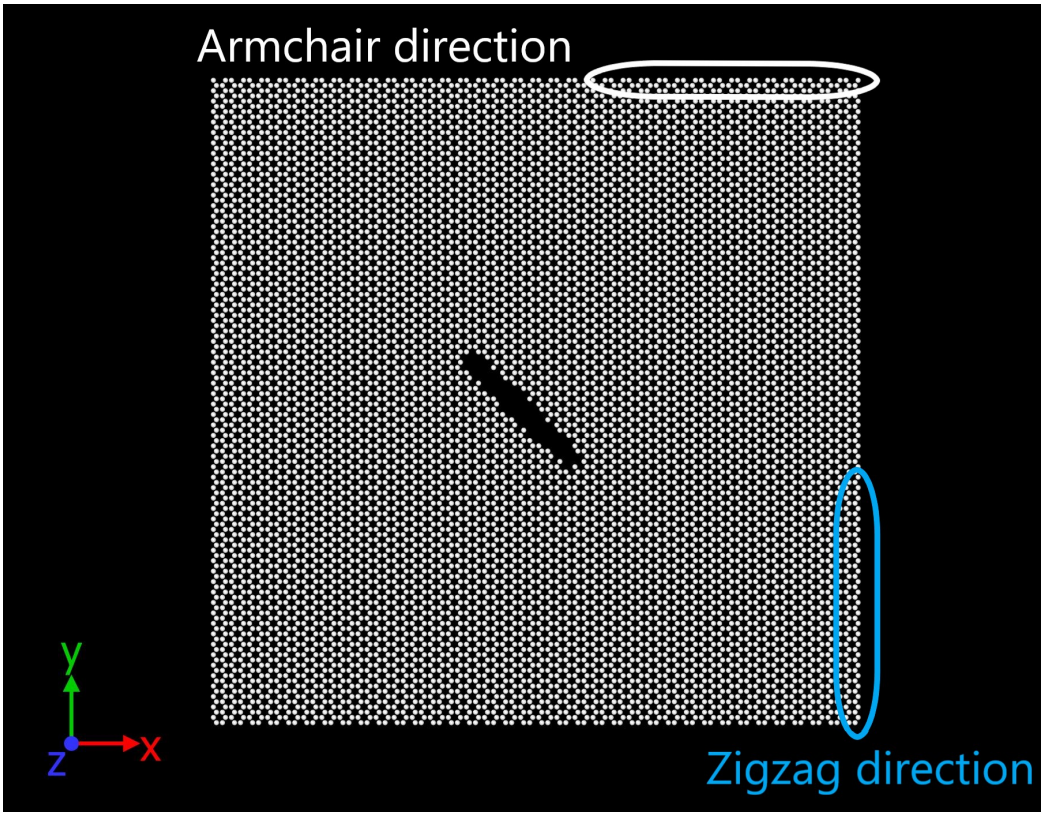

Figure 2.2: GNR with a pre-crack oriented at 45°.

direction, hence it is also called zigzag graphene. We have used AIREBO potential for our simulation because it is commonly used for graphene simulations and captures the physics better than other potentials available.[12] Metal units are used for all the simulations. Berendsen thermostat is used to carry out all the simulations at room temperature (300K). The timestep given is 0.001 ps and the displacement rate of the top layer of carbon atoms is 0.01 A°s^{-1}.

2.2 Griffith's brittle fracture

Zhang, P., Ma, L., Fan, F. et al. have shown that the classic Griffith theory of brittle fracture applies to graphene.[13] The Griffith's criterion for a central crack of length $2a_0$ is given by,

$$\sigma_c = \sqrt{2\gamma E/\pi a_0} \tag{2.1}$$

where σ_c is the stress at fracture, E is Young's modulus, a_0 is the half-length of the crack, and γ is the edge energy. This criterion is used to validate the simulation results later in this report.

Chapter 3

Results and Discussion

The final image of the MD simulation obtained from OVITO is shown along with the stress-strain curve in the results below for the corresponding ten angles. The stress values are then used to calculate the critical stress intensity factor of fracture, K_c. Later, the K_c's of all ten GNR are then compared with the published results for validation.

The stress in the images is stress in the Y direction because we are displacing the nanoribbon in the positive y-direction. Rainbow scale is chosen to visualize the stress, where red is the highest, green is in the middle, and blue is the lowest.

MATLAB is used to plot all the stress-strain curves.[14] The displacement rate of the top layer of GNR is taken to be the value that corresponds to clear crack propagation.

3.1 GNR with a pre-crack oriented at 0°

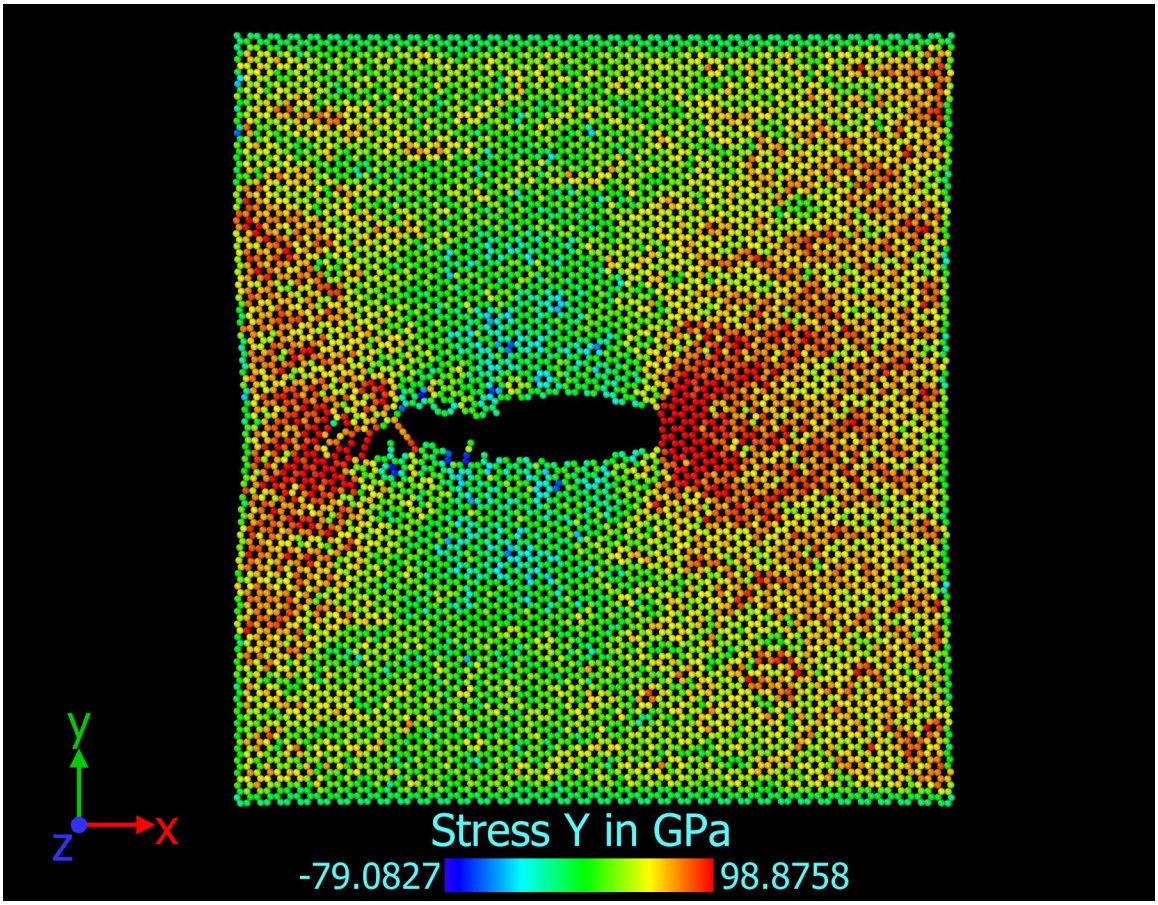

Figure 3.1: Crack propagation in GNR with a pre-crack at 0°.

3.2 GNR with a pre-crack oriented at 5°

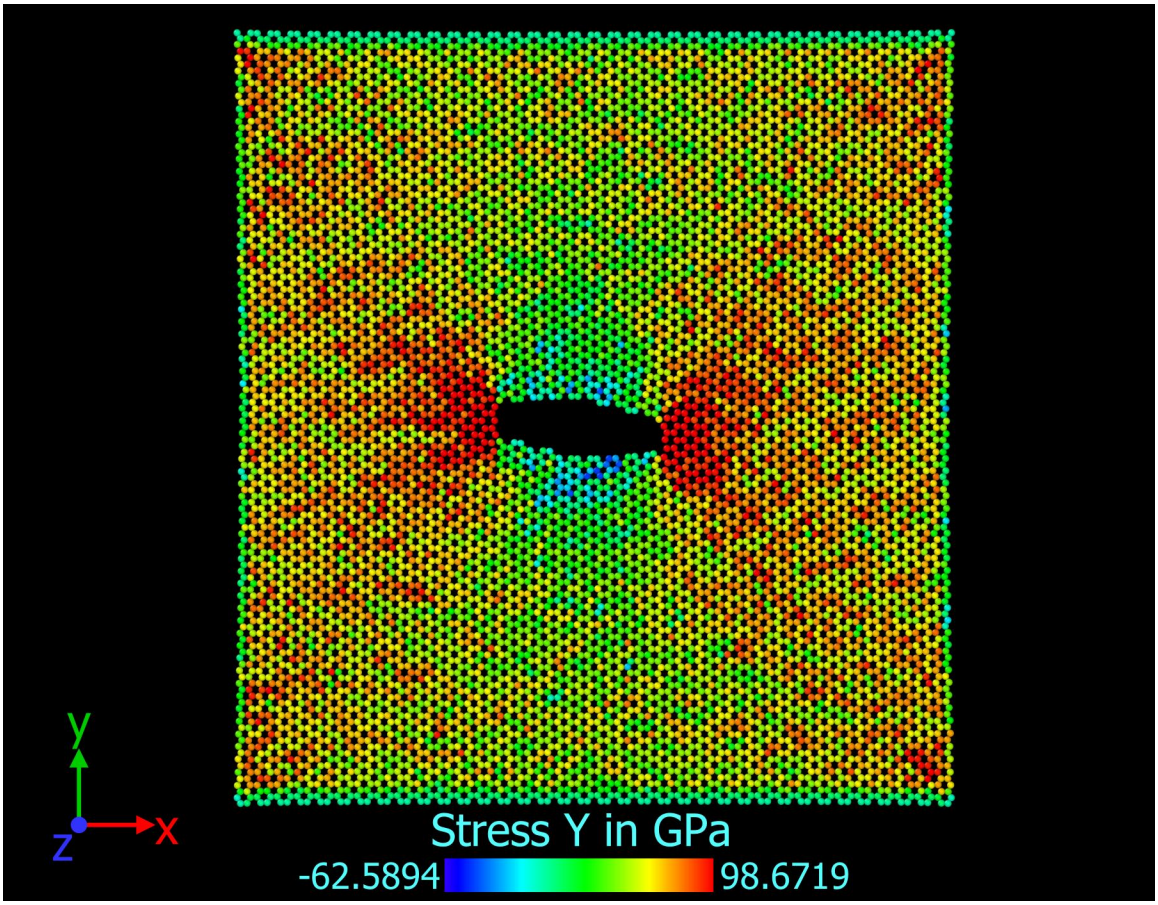

Figure 3.2: Crack propagation in GNR with a pre-crack at 5°.

3.3 GNR with a pre-crack oriented at 10°

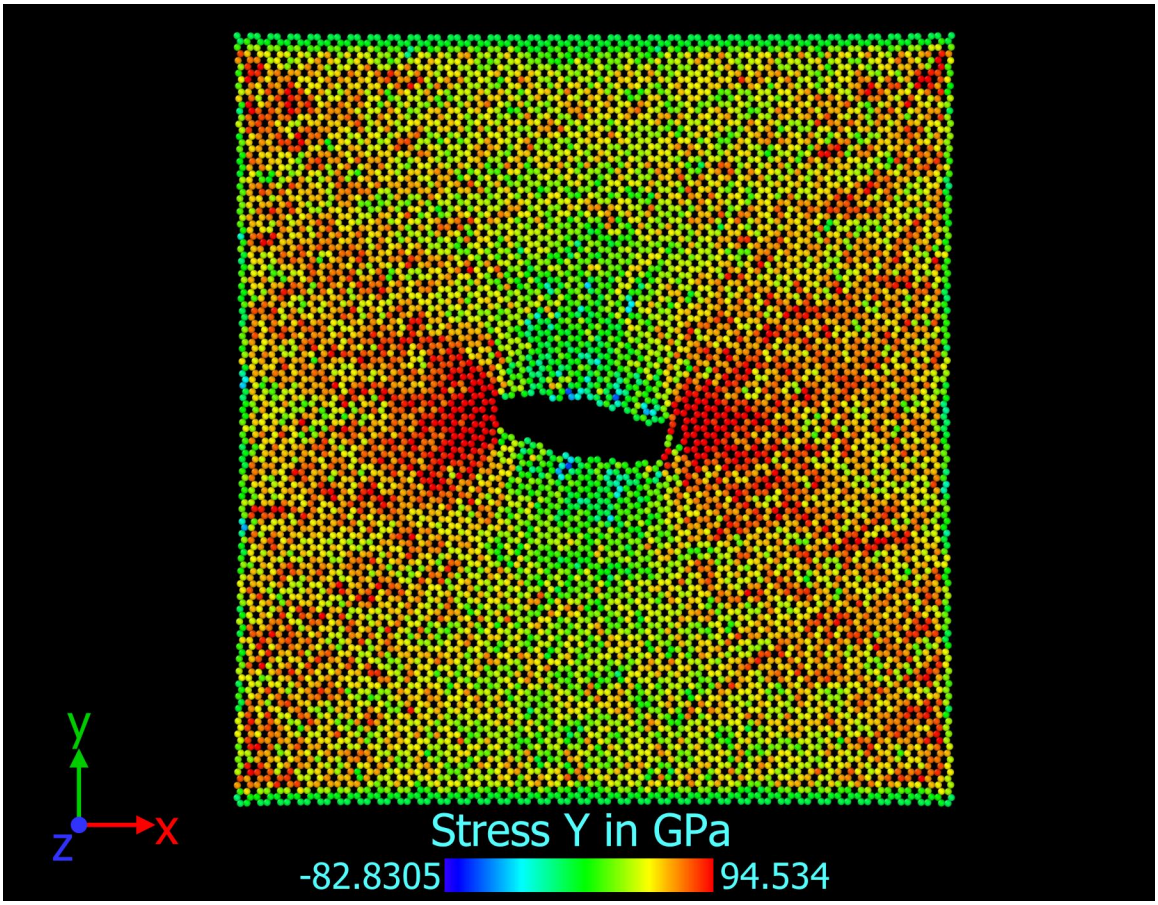

Figure 3.3: Crack propagation in GNR with a pre-crack at 10°.

3.4 GNR with a pre-crack oriented at 15°

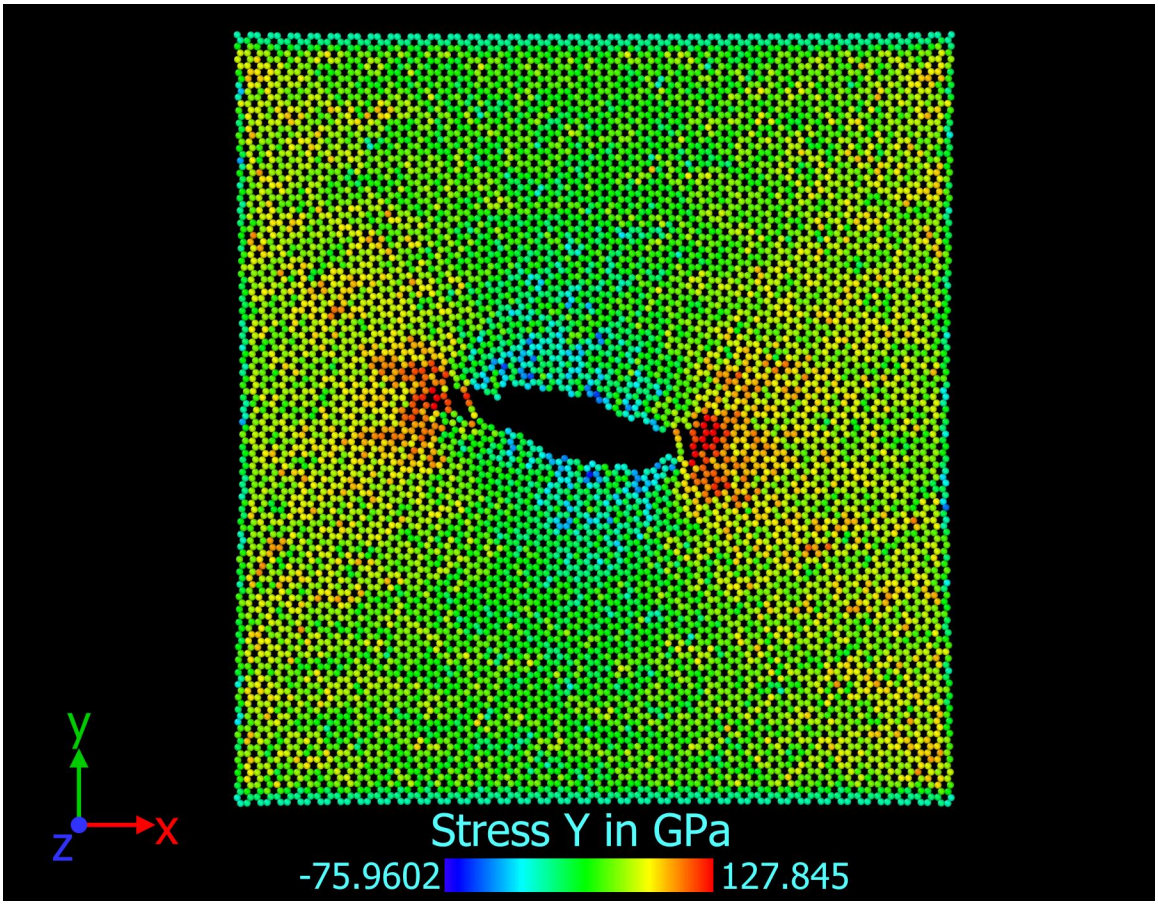

Figure 3.4: Crack propagation in GNR with a pre-crack at 15°.

3.5 GNR with a pre-crack oriented at 20°

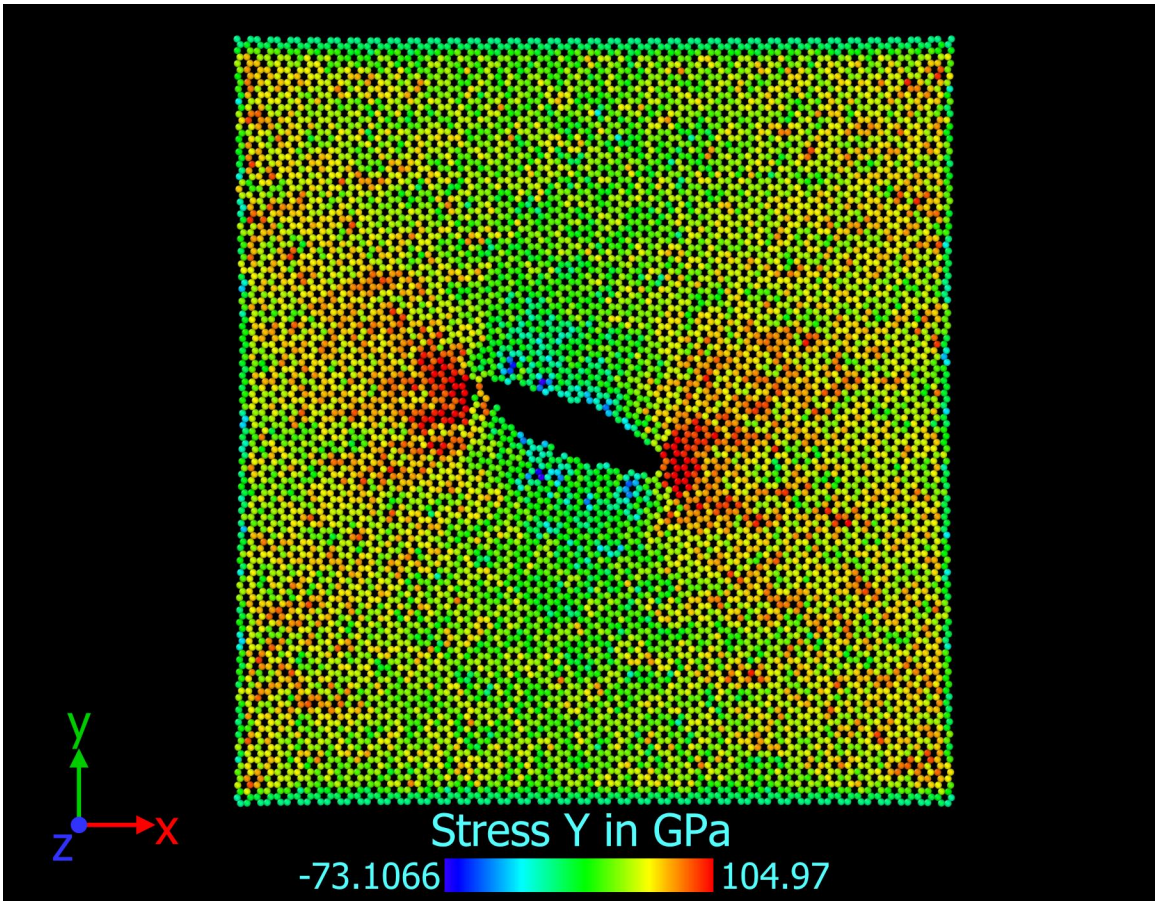

Figure 3.5: Crack propagation in GNR with a pre-crack at 20°.

3.6 GNR with a pre-crack oriented at 25°

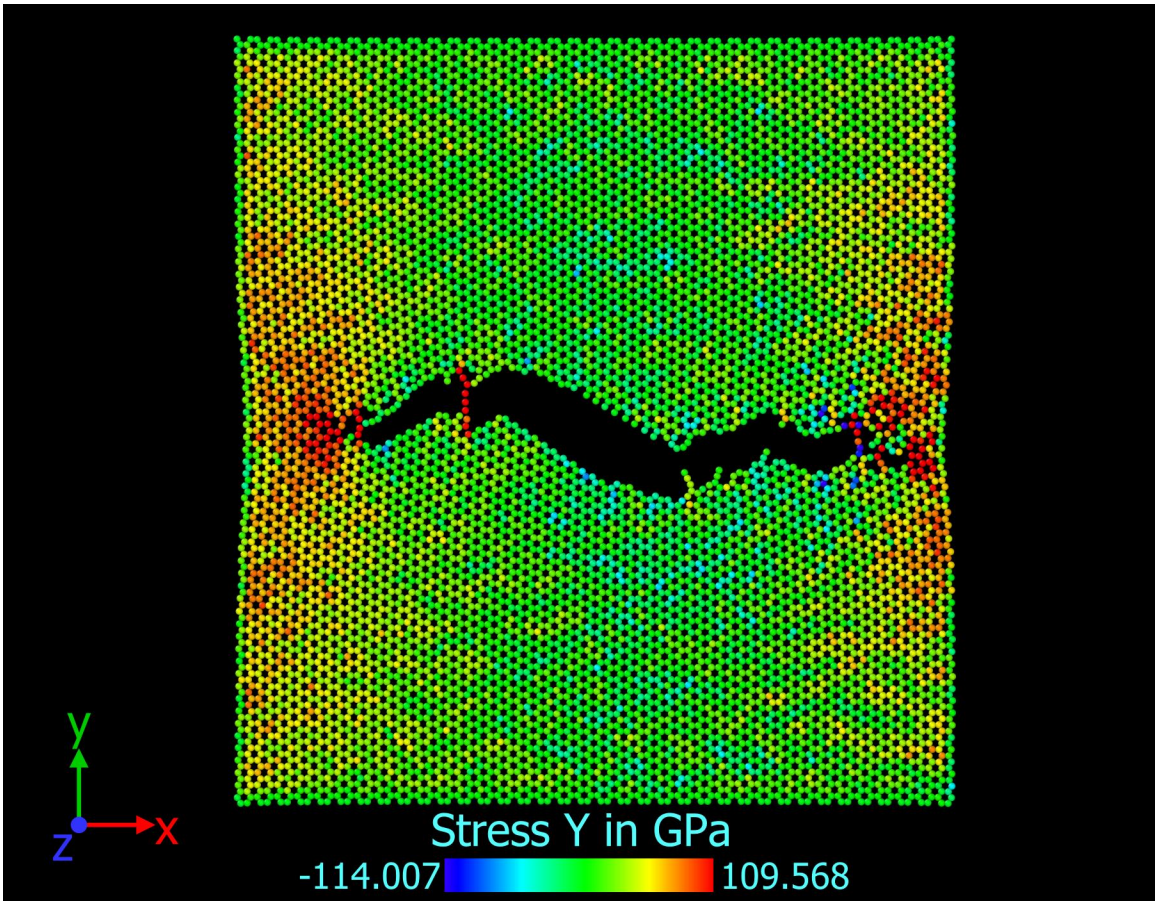

Figure 3.6: Crack propagation in GNR with a pre-crack at 25°.

3.7 GNR with a pre-crack oriented at 30°

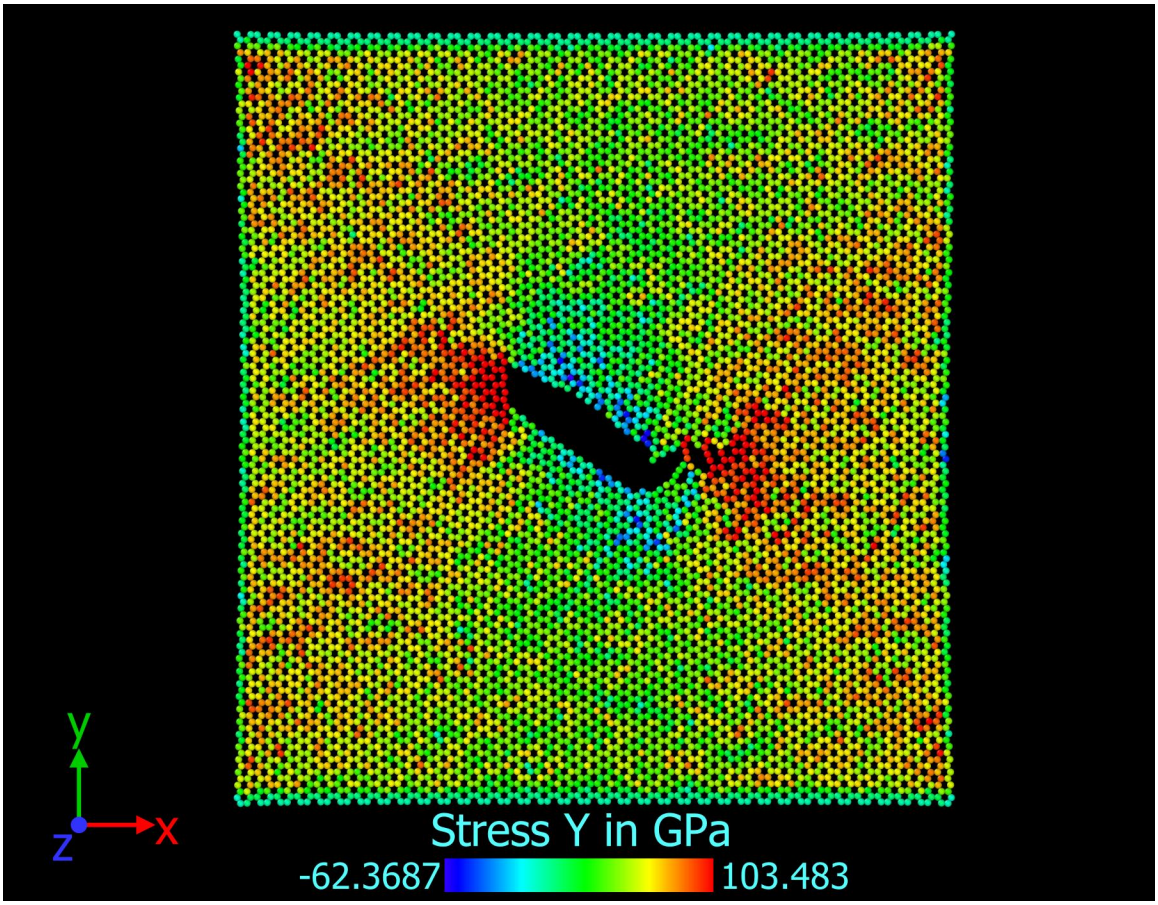

Figure 3.7: Crack propagation in GNR with a pre-crack at 30°.

3.8 GNR with a pre-crack oriented at 35°

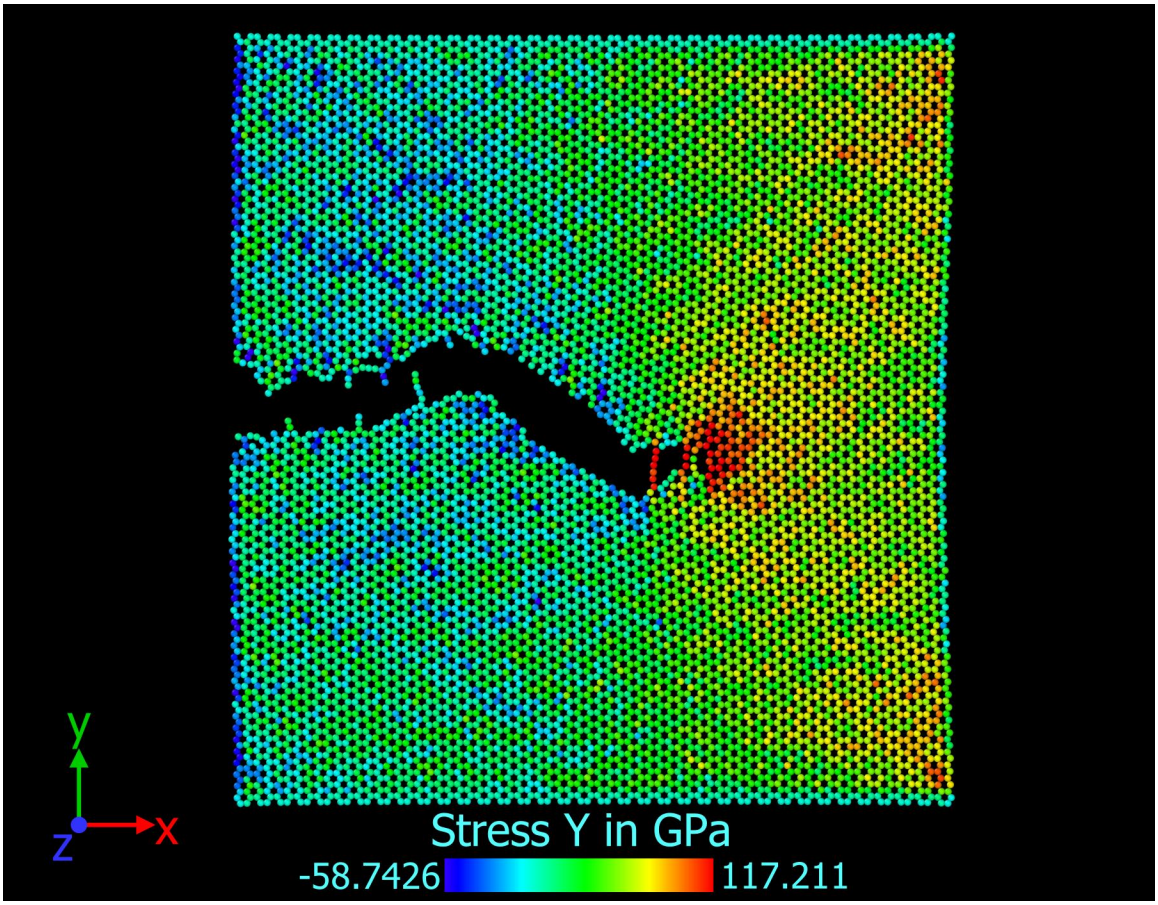

Figure 3.8: Crack propagation in GNR with a pre-crack at 35°.

3.9 GNR with a pre-crack oriented at 40°

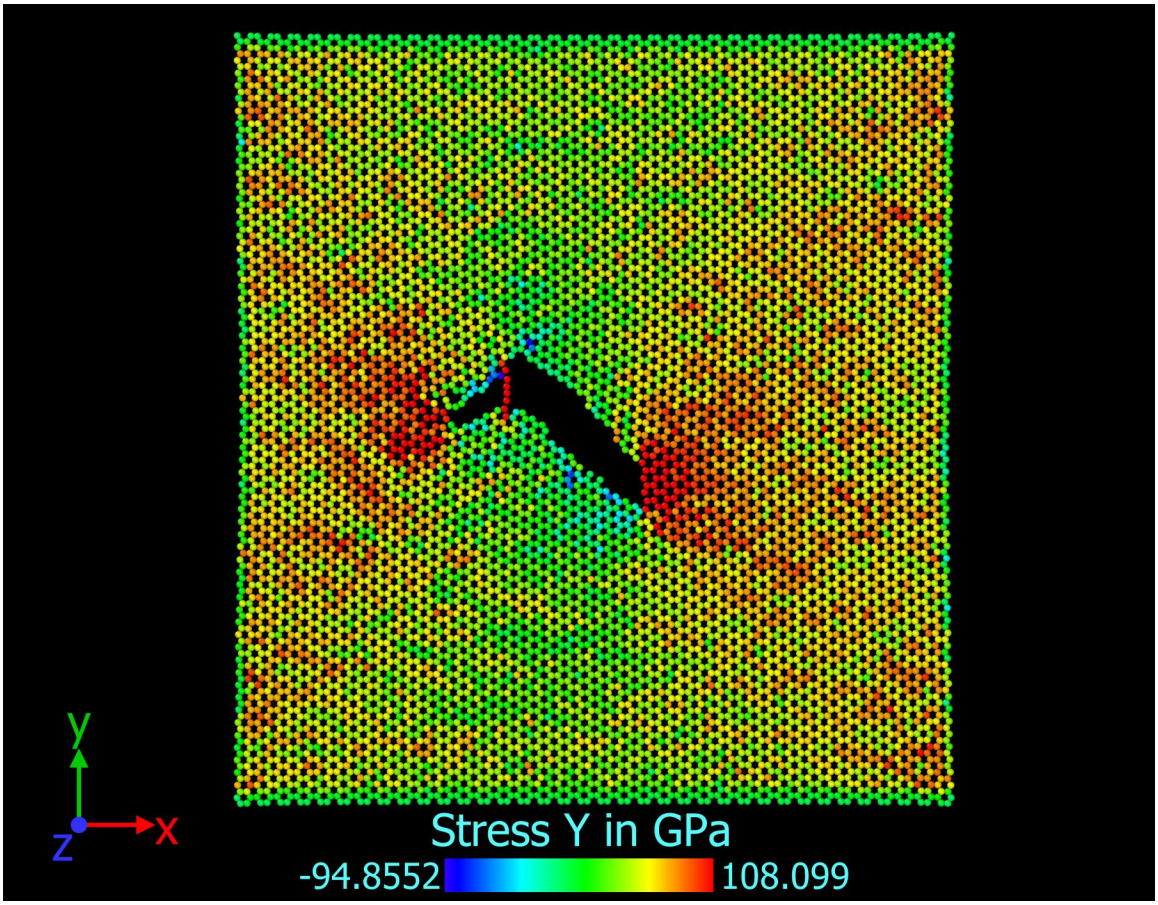

Figure 3.9: Crack propagation in GNR with a pre-crack at 40°.

3.10 GNR with a pre-crack oriented at 45°

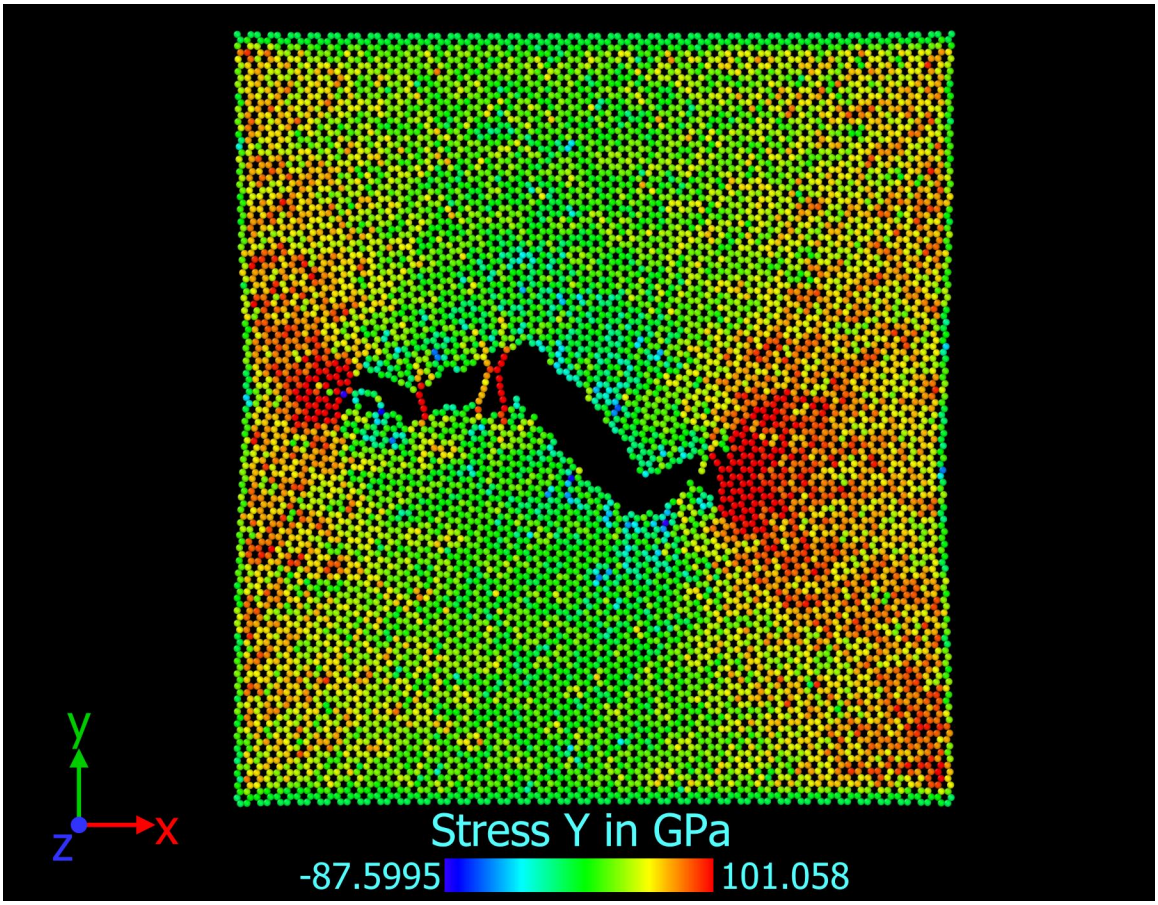

Figure 3.10: Crack propagation in GNR with a pre-crack at 45°.

3.11 Virial stress computation in LAMMPS

Virial stress computation as mentioned in Dr. Dibakar Datta's PhD thesis is given by equation 3.1.[15] For homogeneous systems, it is a measure of mechanical stress

on molecular level.

$$\left\langle \sigma_{ij}^{V} \right\rangle = \frac{1}{2V} \sum_{k=1}^{N} \sum_{l \neq k}^{N} \left(x_i^l - x_i^k \right) f_j^{kl(\text{ int })} - \frac{1}{V} \sum_{k=1}^{N} x_i^k \left(f_j^{k(ext)} - m^k \ddot{x}_j^k \right) \tag{3.1}$$

The virial stress computation in LAMMPS for an atom numbered 1 is given by equation 3.2.[15] The six components of a symmetric tensor is genereated when a and b take on the values x, y, and z.

$$\begin{aligned} S_{ab} = -\Bigg[& m v_a v_b + \frac{1}{2} \sum_{n=1}^{N_p} \left(r_{1_a} F_{1_b} + r_{2_a} F_{2_b} \right) + \frac{1}{2} \sum_{n=1}^{N_b} \left(r_{1_a} F_{1_b} + r_{2_a} F_{2_b} \right) + \\ & \frac{1}{3} \sum_{n=1}^{N_a} \left(r_{1_a} F_{1_b} + r_{2_a} F_{2_b} + r_{3_a} F_{3_b} \right) + \frac{1}{4} \sum_{n=1}^{N_d} \left(r_{1_a} F_{1_b} + r_{2_a} F_{2_b} + r_{3_a} F_{3_b} + r_{4_a} F_{4_b} \right) + \\ & \frac{1}{4} \sum_{n=1}^{N_i} \left(r_{1_a} F_{1_b} + r_{2_a} F_{2_b} + r_{3_a} F_{3_b} + r_{4_a} F_{4_b} \right) + \text{Kspace} \left(r_{i_a}, F_{i_b} \right) + \sum_{n=1}^{N_f} r_{i_a} F_{i_b} \Bigg] \end{aligned} \tag{3.2}$$

This formulation is in pressure(stress) $\times$ volume units. To convert it into units of stress, we need to divide it by volume per-atom. But in a deformed structure, the volume per-atom is ill defined. So, to get total pressure of the system, the sum of diagonal elements of stress tensor of individual atoms for all atoms in the system is divided by the product of dimension and volume of the system.[15] So, to get stress in GPa, we take a product of LAMMPS value and a multiplication factor.

Multiplication factor is given by 1/volume per-atom $\times$ 1e-4 (1 bar = 1e-4 GPa). We

have 8860 atoms and size of the nanoribbon is 150 × 150 A°. So, volume per-atom in this work is 8.66 °A^3. In our case the multiplication factor is 1.155e-5.[15]

3.12 Stress-Strain curve

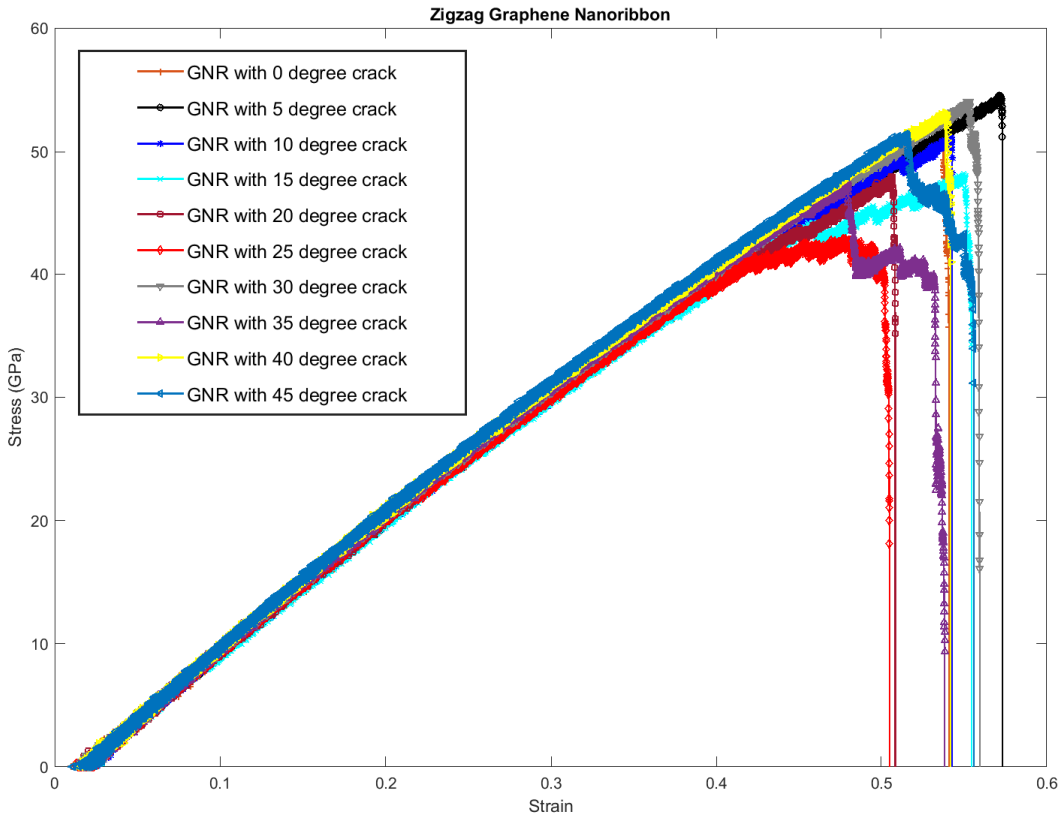

Figure 3.11: Stress-strain curve for all GNRs

The strain values in the Figure 3.11 look higher than expected, but it is dependent on the rate at which the nanoribbon is pulled. In this work, this is checked through varying the rate of displacement and observing the change in values of stress at

fracture. No significant change in values of stress at fracture was found, and the rate at which we get a clear crack propagation was taken.

3.13 Validation

From Zhang, P., Ma, L., Fan, F. et al, the average value of K_c obtained is 4.0 MPa$\sqrt{m}$, with a standard deviation of 0.6 MPa$\sqrt{m}$.[13] In Table 3.1, this value is compared with K_c values for all ten cracked GNRs. K_c is equal to $\sigma_c \sqrt{\pi a_0}$.[13]

Table 3.1
Calculated K_c values corresponding to their crack angles

crack angle	0	5	10	15	20	25	30	35	40	45
K_c	3.48	3.69	3.45	3.23	3.2	2.9	3.65	3.17	3.59	3.48

According to Griffith's criterion, the product of σ_c and $\sqrt{a_0}$ has to be constant. $\sigma_c \sqrt{a_0}$ range in the referred article is 1.73 to 2.78 MPa$\sqrt{m}$. In this report, only the 25° crack has a value of 1.64 MPa$\sqrt{m}$ that goes below the given range. Hence, the simulation results are in accordance with the published results. Table 3.2 contains $\sigma_c \sqrt{a_0}$ values for all ten GNRs.

Table 3.2
Calculated $\sigma_c \sqrt{a_0}$ values corresponding to their crack angles

crack angle	0	5	10	15	20	25	30	35	40	45
$\sigma_c \sqrt{a_0}$	1.96	2.08	1.95	1.82	1.8	1.64	2.06	1.79	2.03	1.96

All the values are around 2 MPa$\sqrt{m}$, so it can be considered as a constant. Hence, Griffith's theory is applicable to graphene.

3.14 Conclusion

After analyzing the results from MD simulations, the crack path can be observed for all ten GNRs. It can be concluded that the GNR with crack at 25° angle has the lowest strength because it has the sharpest crack tip and slightly different crack shape than other GNRs. This conclusion is specific for a particular crack length. It can also be said that the crack path depends on the length of the crack, orientation of the crack, crack tip sharpness, and also the shape of the crack.

3.15 Future work

Since MD simulations are computationally expensive, our future work involves prediction of fracture in graphene using Deep Learning. The goal is to reduce the time required in making fracture path predictions by bypassing MD simulations with a machine learning model.

References

[1] Wikimedia. AlexanderAlUS. **2010**.

[2] Büyüköztürk, O.; Buehler, M. J.; Lau, D.; Tuakta, C. *International Journal of Solids and Structures* **2011**, *48*(14), 2131–2140.

[3] Lee, C.; Wei, X.; Kysar, J.; Hone, J. *Science* **2008**, *321*, 385–388.

[4] Balandin, A.A.and Ghosh, S.; Bao, W.; Calizo, I.; Teweldebrhan, D.; Miao, F.; Lau, C. *Nano Letters* **2008**, *8*, 902–907.

[5] Ho, Y. H.; Wu, J. Y.; Chiu, Y. H.; Wang, J.; Lin, M. F. *Royal Society* **2010**, *368*, 5353–5354.

[6] Wahl, L.; Maas, S.; Waldmann, D.; Zürbes, A.; Frères, P. *Journal of Sandwich Structures & Materials* **2012**, *14*, 449–468.

[7] Molecular dynamics — Wikipedia, the free encyclopedia. Wikipedia contributors. **2021**.

[8] Datta, D.; Nadimpalli, S. P.; Li, Y.; Shenoy, V. B. *Extreme Mechanics Letters* **2015**, *5*, 10–17.

[9] Plimpton, S. *Journal of Computational Physics* **1995**, *117*, 1–19.

[10] Stukowski, A. JAN **2010**, *18*(1).

[11] Pei, Q.; Zhang, Y.; Shenoy, V. *Carbon* **2010**, *48*(3), 898–904.

[12] Stuart, S. J.; Tutein, A. B.; Harrison, J. A. *The Journal of Chemical Physics* **2000**, *112*(14), 6472–6486.

[13] Zhang, P.; Ma, L.; Fan, F.; Zeng, Z.; Peng, C.; Loya, P. E.; Liu, Z.; Gong, Y.; Zhang, J.; Zhang, X.; Ajayan, P. M.; Zhu, T.; Lou, J. *Nat Commun* **2014**, *5*, 3782.

[14] MATLAB. *version 9.8.0.1538580 (R2020a);* The MathWorks Inc.: Natick, Massachusetts, 2020.

[15] Datta, D. *Topics in Mechanics at the Bottom, Energy StorageSystems, and Emerging Nanomaterials* PhD thesis, Brown University, **2015**.